

APPENDIX J
DESCRIPTION OF UNCERTAINTY CALCULATIONS



THIS PAGE INTENTIONALLY LEFT BLANK



1
2
3
4
5
6
7
8
9
10
11
12
13
14
15
16
17
18
19
20
21
22
23
24
25
26
27
28
29
30
31
32
33
34
35
36
37
38
39
40
41
42
43
44
45
46
47
48
49

DESCRIPTION OF UNCERTAINTY CALCULATIONS

1.0 MONTE CARLO SAMPLING WITH THE STADIC CODE

1.1 General Description

The Monte Carlo technique maps uniform, random numbers through a cumulative distribution function (CDF) of a physical or decision parameter of the FORTRAN code to generate a value of that parameter for use in the analysis. Given a uniform density of random deviates on the ordinate, n , the total number of random deviates on any interval, dy , is $n(dy)$. The corresponding interval on the abscissa then has density $n(dy/dx)$. Since the probability density function (PDF) of a random variable is proportional to the derivative of the corresponding CDF, this method of mapping uniform deviates through the CDF, in effect, simulates the PDF of the random variable.

The STADIC code was developed by PLG to accomplish Monte Carlo sampling for engineering oriented applications. The STADIC code has been certified under QA and is used by PLG as a production code on the PC. It is designed to generate values of input parameters from user specified distributions and pass them to a subroutine for calculation. The results of each iteration is then stored for statistical and trend analysis. Thus, STADIC automates the Monte Carlo technique by providing a convenient platform to run standard FORTRAN engineering code. Further information on the code can be found in Wakefield and Fleming (1990).

1.2 Description of STADIC Subroutine for EA Evaluations

The STADIC subroutine specifies the probability distributions to be sampled for use in the Design Analysis Model (DAM) calculation cases. The code has the capability to accept the parameters for some of the standard distributions used in this study. These include those parameters that specify normal, lognormal, uniform, and discrete distributions. Other distributions (such as piece wise continuous and triangular distributions) are converted into CDFs for input to the Monte Carlo algorithms in the STADIC code.

Dependencies are established by standard FORTRAN programming. For example, full dependence corresponds to use of the same random number to sample the two separate CDFs for the dependent variables. The subroutine first queries the Monte Carlo random number generator with an intermediate variable corresponding to a uniform distribution between 0 and 1. It then uses the resulting value to select a sample value from the CDFs of each of the dependent variables.

For the Engineered Alternatives (EA) Cost Effectiveness Study, the STADIC code was used to generate a file consisting of 1,000 sets of input for the uncertain variables, indexed from 1 to 1,000. The modeling of the probability distributions for these variables is discussed in Section 2.0 of this appendix. The input file was then used to run 1,000 iterations of the DAM code. One set of input initiated a 10,000 year calculation in the DAM. The results of each calculation were then saved with the index number corresponding to the input set. In this manner the output of each DAM calculation can be easily correlated with its input set for calculation of Measures of Relative Effectiveness (MRE) and examination of sensitivities to obtain physical insight into the influence of the EA on performance.



1 The same random number seed was used to generate the input set for the baseline and all the
2 EAs. This insured that the "unknown future conditions" that sampling process simulates is
3 consistent across all the EA options so that the relative response of the to the conditions can be
4 compared. Thus, the uncertainty associated with the resultant MRE may be considered to be due
5 to the uncertainty in our state-of-knowledge regarding physical processes under those future
6 conditions and not the nature of the random sampling process.
7

8 9 **2.0 INPUT PARAMETER DISTRIBUTIONS**

10 11 12 **2.1 Summary of Uncertain Parameters Modeled**

13
14 This section summarizes the modeling of the DAM parameters whose uncertainties were
15 considered important to determining the significance of the various for improving confidence of
16 compliance. Table J-1 provides summary information regarding these parameters and references
17 to the sources of evidence used to establish their probability distributions.
18

19 Figure J-1(a-p) presents a graphical representation of the cumulative distribution functions
20 generated by the STADIC code for the baseline design. The graphs are presented in the same
21 order as they are listed in Table J-1. As a matter of clarification, the graphs of hydrogen
22 generation rate under humid conditions (HHUMRATE) and negative log permeability of the
23 anhydrite units (KPANH) appear to be step functions. This reflects the fact that these two
24 variables are discrete distributions. For example, all random numbers between 0 and 0.2 would
25 return a value of 17 for KPANH.
26

27 **2.2 Dependencies Among Variables**

28
29 The following dependencies and correlations among input parameters are modeled in the STADIC
30 sampling subroutine:
31

- 32 • Inundated and Humid anoxic corrosion gas generation rates: The same random
33 number is used to sample the distributions for the variables HINURATE and
34 HHUMRATE that represent these two processes. These two processes could
35 proceed in parallel within the repository, depending on the amounts of brine
36 available for the conversion reaction. The dependency reflects the similarity of the
37 chemical conversion involved, with the differences in brine saturation producing a
38 different model for the rate of the process. The use of the same random number
39 for the two processes reflects the judgement that the humid gas generation rate
40 should never exceed the inundated anoxic gas generation rate, since the cumulative
41 distribution of the humid process has lower values at all percentiles of the
42 distribution.
43
- 44 • Inundated and Humid biodegradation gas generation rates: The same random
45 number is used to sample the distributions for the variables BINURATE and
46 BHUMRATE that represent these two processes. These two processes could
47 proceed in parallel within the repository, depending on the amounts of brine
48 available for the conversion reaction. The dependency reflects the similarity of the
49 chemical conversion involved, with the differences in brine saturation producing a



TABLE J-1

INPUT VARIABLES TO THE DAM THAT ARE MODELED WITH UNCERTAINTY

DAM Variable Name	Variable Description (units)	Point Estimate ^a	Range of Values ^b	Type of Distribution	Dependencies	Comments	Reference
BHUMRATE	Microbial gas generation rate under humid facility conditions (moles/kg cellulose-yr)	0.01	0 - 0.1	Piece-wise Uniform	BINURATE >= BHUMRATE	Range of values above and below point estimate weighted to make overall mean value of distribution equal to the point estimate.	Brush, 1994, and SNL/NM, 1993, Vol. 3, p. 3-52
BINURATE	Microbial gas generation rate from anoxic corrosion under inundated facility conditions (moles/kg cellulose-yr)	0.1	0 - 0.5	Piece-wise Uniform	BINURATE >= BHUMRATE	Range of values above and below point estimate weighted to make overall mean value of distribution equal to the point estimate.	Brush, 1994, and SNL/NM, 1993, Vol. 3, pp. 3-50, 3-51
BIOSTOIC	Ratio of moles of biogas generated to moles of cellulose consumed (dimensionless)	0.835	0 - 1.67	Uniform	None		See Note h.
CB	Brine inflow rate at a pressure difference of lithostatic minus atmospheric (m ³ /yr-panel)	0.60	0 - 1.19	Uniform	None		See Note h.
H2MAX	Maximum hydrogen gas generation potential from anoxic corrosion (mol/panel)	7.9E+07	5.5E7 - 1.1E8	Derived distribution	Derived directly from RHTORW.	H2MAX=H2MAX0*RHTORW/0.7 See comments for variable RHTORW.	See Note g.
HHUMRATE	Hydrogen gas generation rate from anoxic corrosion under humid facility conditions (moles/drum-yr)	9.0E-04	0 - 0.06	Discrete	HINURATE >= HHUMRATE	Three values assigned the following weights: 97.5% @ 0.0, 2% @ 0.03, 0.5% @ 0.06 See Note i	Brush, 1994, and SNL/NM, 1993, Vol. 3, pp. 3-46, 3-47
HINURATE	Hydrogen gas generation rate from anoxic corrosion under inundated facility conditions (moles/drum-yr)	0.6	0 - 10	Piece-wise Uniform	HINURATE >= HHUMRATE	Range of values above and below point estimate weighted to make overall mean value of distribution equal to the point estimate.	Brush, 1994, and SNL/NM, 1993, Vol. 3, pp. 3-44, 3-45
KPANH	Negative log of the permeability of the anhydrite beds (dimensionless)	18	17,18,19,20	Discrete	None	Due to DAM code, probability assigned to 17,18,19, or 20 only. Assigned equal probability weight.	See Note f.

Refer to footnotes at end of table.

TABLE J-1 (Continued)

INPUT VARIABLES TO THE DAM THAT ARE MODELED WITH UNCERTAINTY

DAM Variable Name	Variable Description (units)	Point Estimate ^a	Range of Values ^b	Type of Distribution	Dependencies	Comments	Reference
RADFAC	Factor used to estimate the effective borehole radius during intrusion (dimensionless)	3.0	2.1 - 3.9	Triangular	None	Range to minimum and maximum values estimated as plus or minus 30% of the point estimate.	See Note g.
RADSOL (1)	Pu-240 solubility in brine (mol/l)	5.01E-04	2E-05 - 0.013	Lognormal ^{c,d}	None		See Note e.
RADSOL (2)	U-236 solubility in brine (mol/l)	3.16E-02	2E-03 - 0.39	Lognormal ^{c,d}	None		See Note e.
RADSOL (3)	Am-241 solubility in brine (mol/l)	3.98E-02	0.0158 - 0.126	Lognormal ^{c,d}	None		See Note e.
RADSOL (5)	Np-237 solubility in brine (mol/l)	2.51E-02	0.005 - 0.158	Lognormal ^{c,d}	None		See Note e.
RADSOL (5)	U-233 solubility in brine (mol/l)	3.16E-02	2E-03 - 0.39	Lognormal ^{c,d}	See comments	Assigned same value as RADSOL (2) and RADSOL (8)	See Note e.
RADSOL (6)	Th-229 solubility in brine (mol/l)	7.94E-08	5E-09 - 1.26E-06	Lognormal ^{c,d}	None		See Note e.
RADSOL (7)	Pu-238 solubility in brine (mol/l)	5.01E-04	2E-05 - 0.013	Lognormal ^{c,d}	See comments	Assigned same value as RADSOL (1) and RADSOL (12)	See Note e.
RADSOL (8)	U-234 solubility in brine (mol/l)	3.16E-02	2E-03 - 0.39	Lognormal ^{c,d}	See comments	Assigned same value as RADSOL (2) and RADSOL (5)	See Note e.
RADSOL (9)	Th-230 solubility in brine (mol/l)	7.94E-08	5E-09 - 1.26E-06	Lognormal ^{c,d}	See comments	Assigned same value as RADSOL (6)	See Note e.
RADSOL (12)	Pu-239 solubility in brine (mol/l)	5.01E-04	2E-05 - 0.013	Lognormal ^{c,d}	See comments	Assigned same value as RADSOL (1) and RADSOL (7)	See Note e.

Refer to footnotes at end of table.

TABLE J-1 (Continued)

INPUT VARIABLES TO THE DAM THAT ARE MODELED WITH UNCERTAINTY

DAM Variable Name	Variable Description (units)	Point Estimate ^a	Range of Values ^b	Type of Distribution	Dependencies	Comments	Reference
RBOR	Radius of borehole for intrusion scenarios (m)	0.18	0.134-0.222	Uniform	None	Distributions taken directly from 92PA due to the lack new data.	Distribution Type and range from SNL/NM, 1993
RHTORW	Ratio of hydrogen gas generation rate to water consumption rate during anoxic corrosion (dimensionless)	0.72	0.5 - 1	Derived Distribution	None	RHTORW=(4-x)/(4+2x) where x is uniform between 0 and 1.	See Note g.

Notes:

^aPoint estimate value is the mean of the distribution for all distribution types except for the lognormal distribution.

^bRange of values represent all possible values of the distribution (0th to 100th percentile) for all distributions except for the lognormal distribution.

^cFor lognormal distribution, the point estimate value is the median.

^dFor lognormal distribution, the range of values is between 5th percentile and 95th percentile.

^ePoint estimate (median) and range values for these variables are taken from Table H-1 Results of Regression Analysis on Actinide Solubility

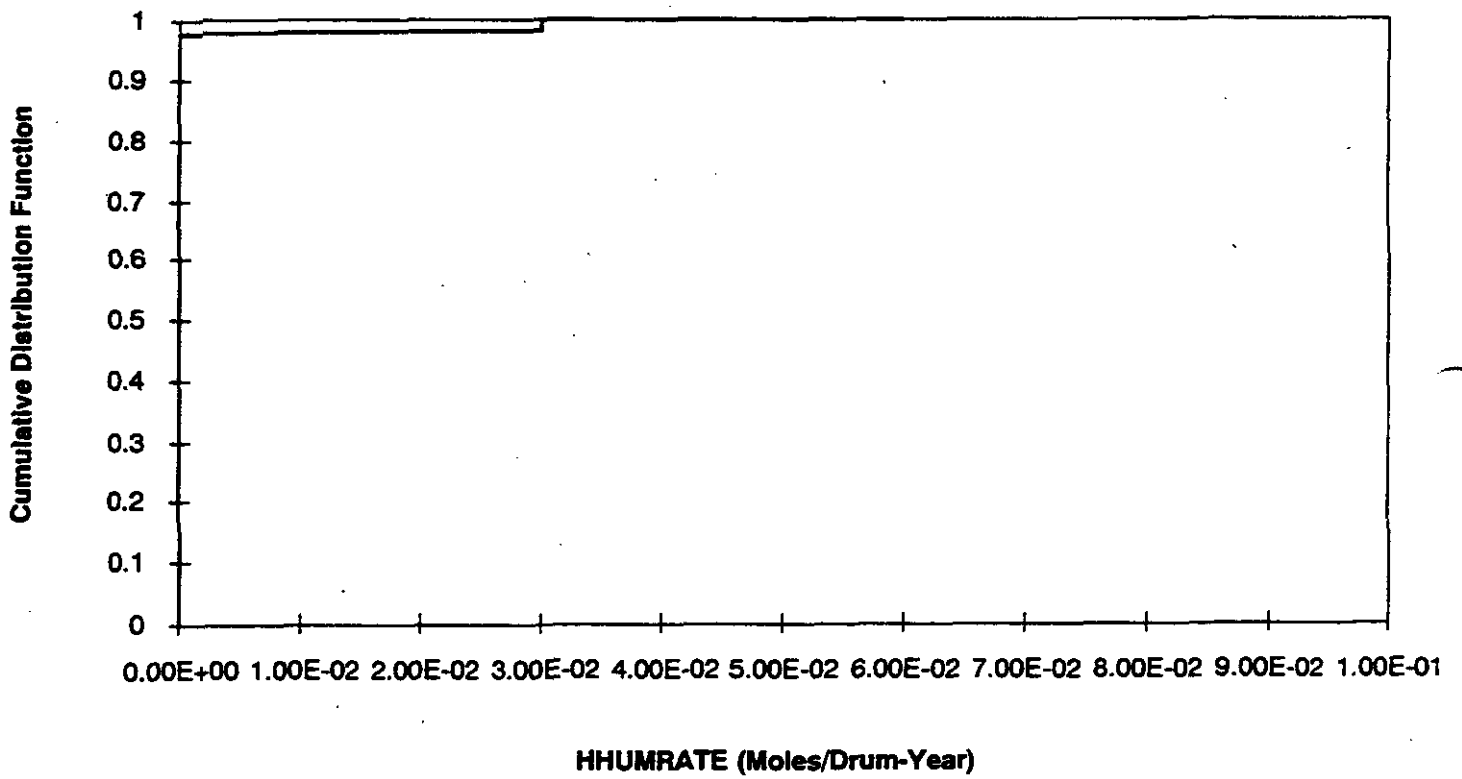
^fKPANH distribution from EATF Report (DOE, 1991).

^gGuidance regarding these variables are taken from equations provided in SNL/NM, 1993.

^hThe complete distributions for these variables are from SNL/NM, 1993, considerations.

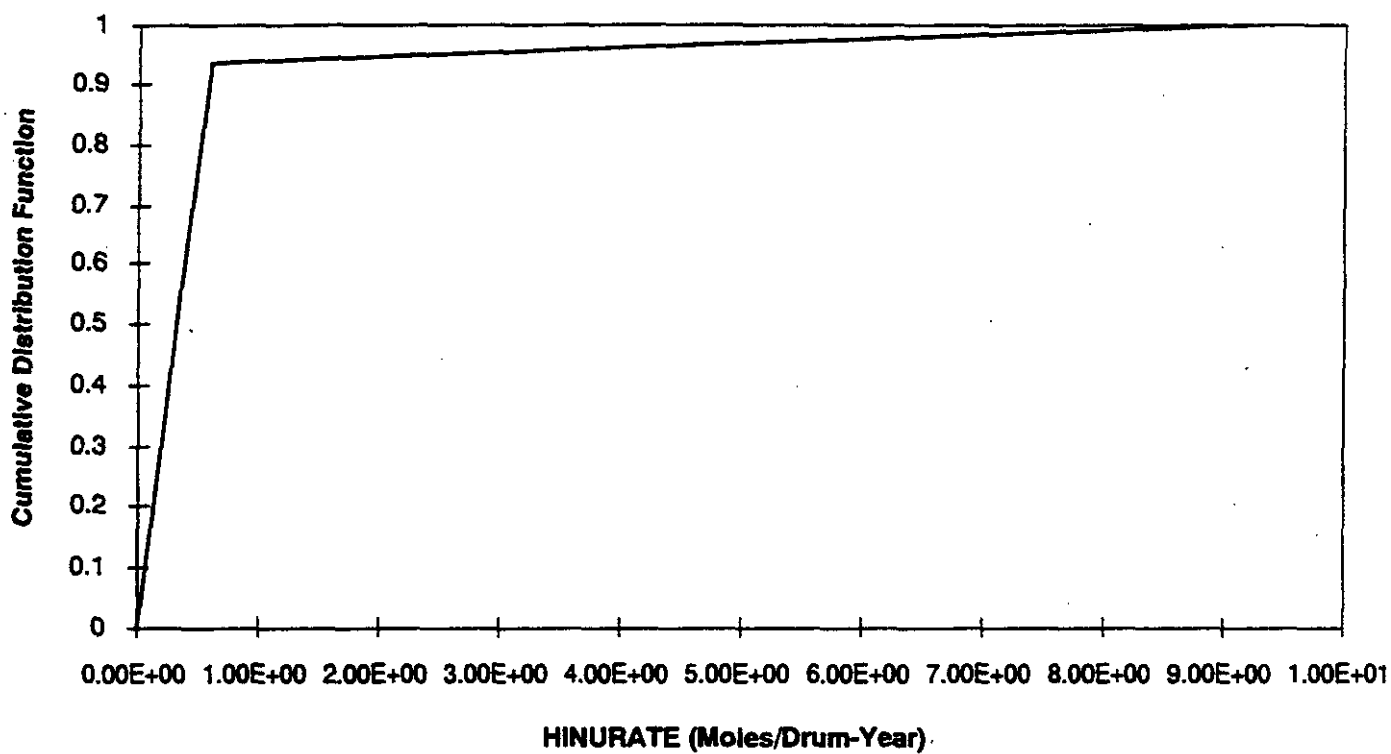
ⁱThis discrete distribution is formulated to recognize that the humid anoxic gas generation rate is very likely zero, but there is some chance that it could be as high as 0.06. Use of discrete distribution would permit examination of a distinct set of cases if an impact is found.





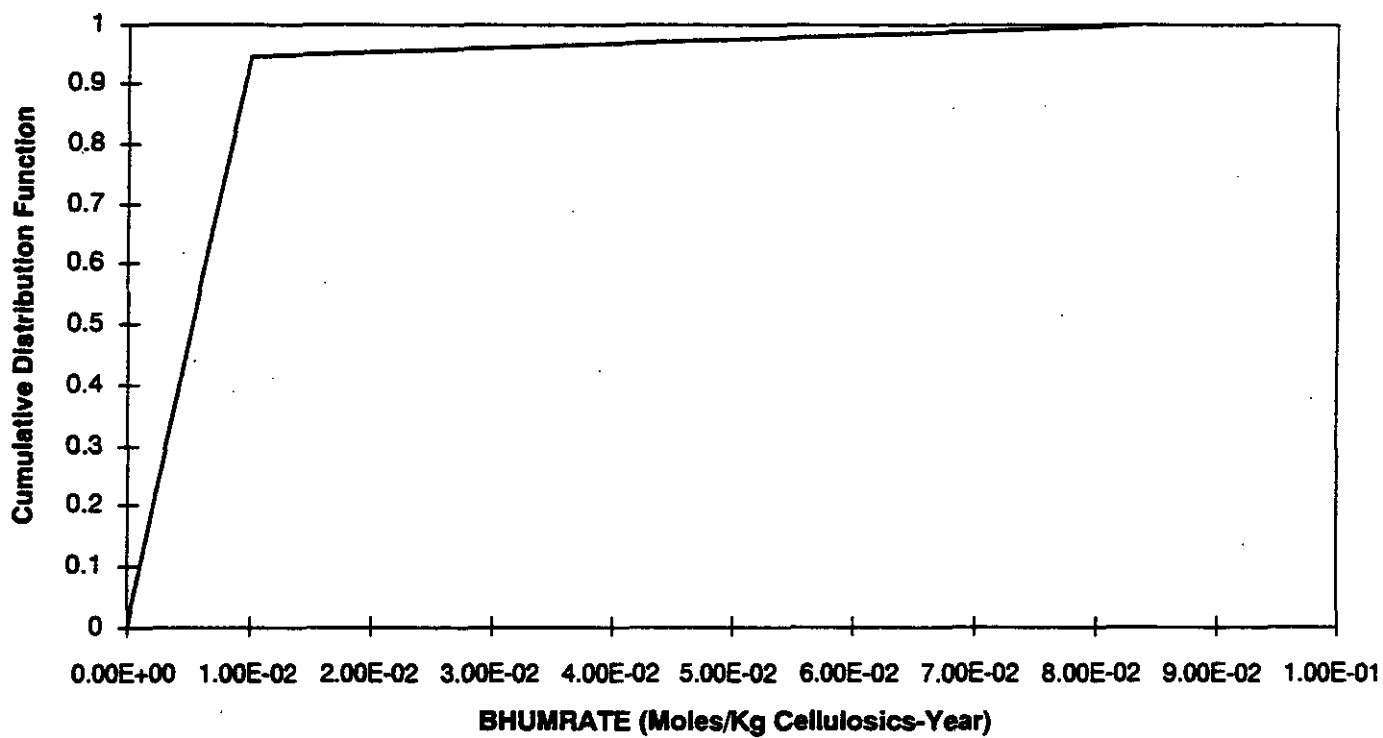
M

Figure J-1a
Cumulative Distribution Function



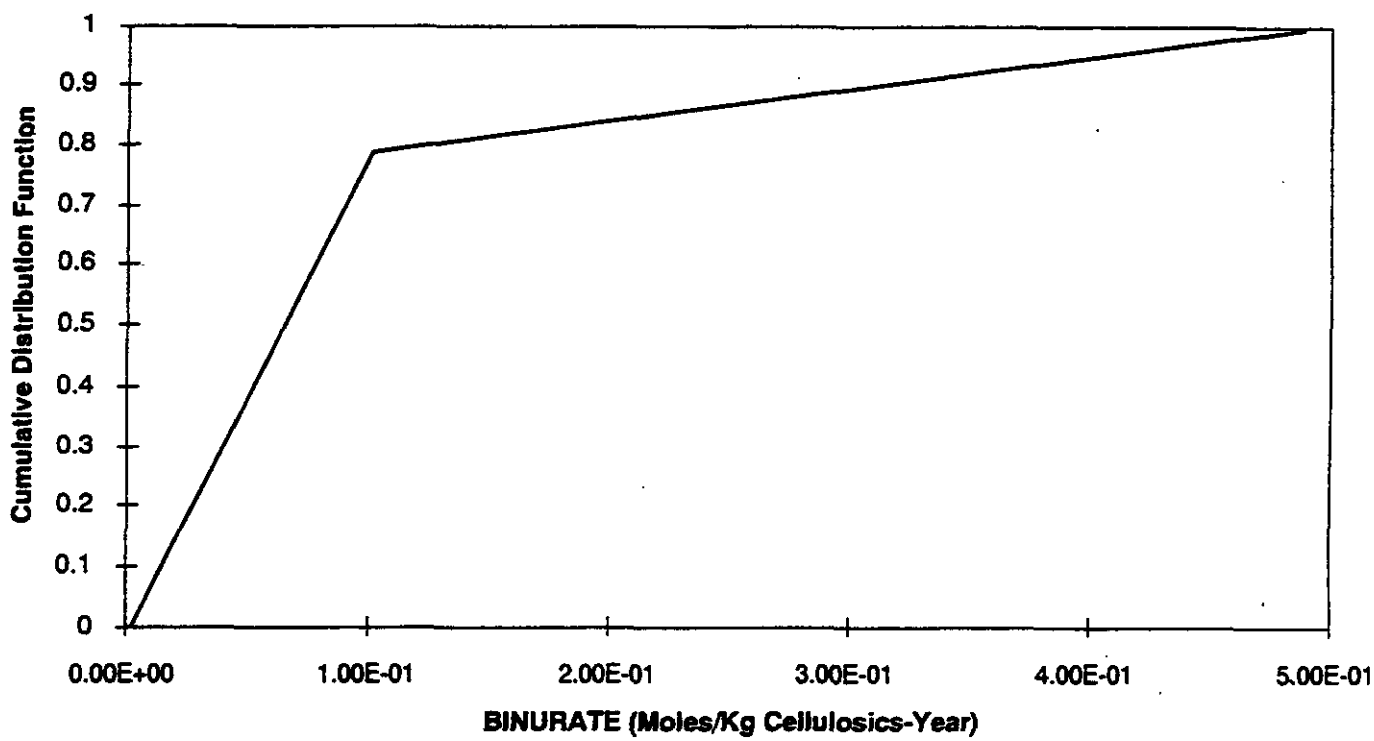
M

Figure J-1b
Cumulative Distribution Function



M

Figure J-1c
Cumulative Distribution Function



M

Figure J-1d
Cumulative Distribution Function

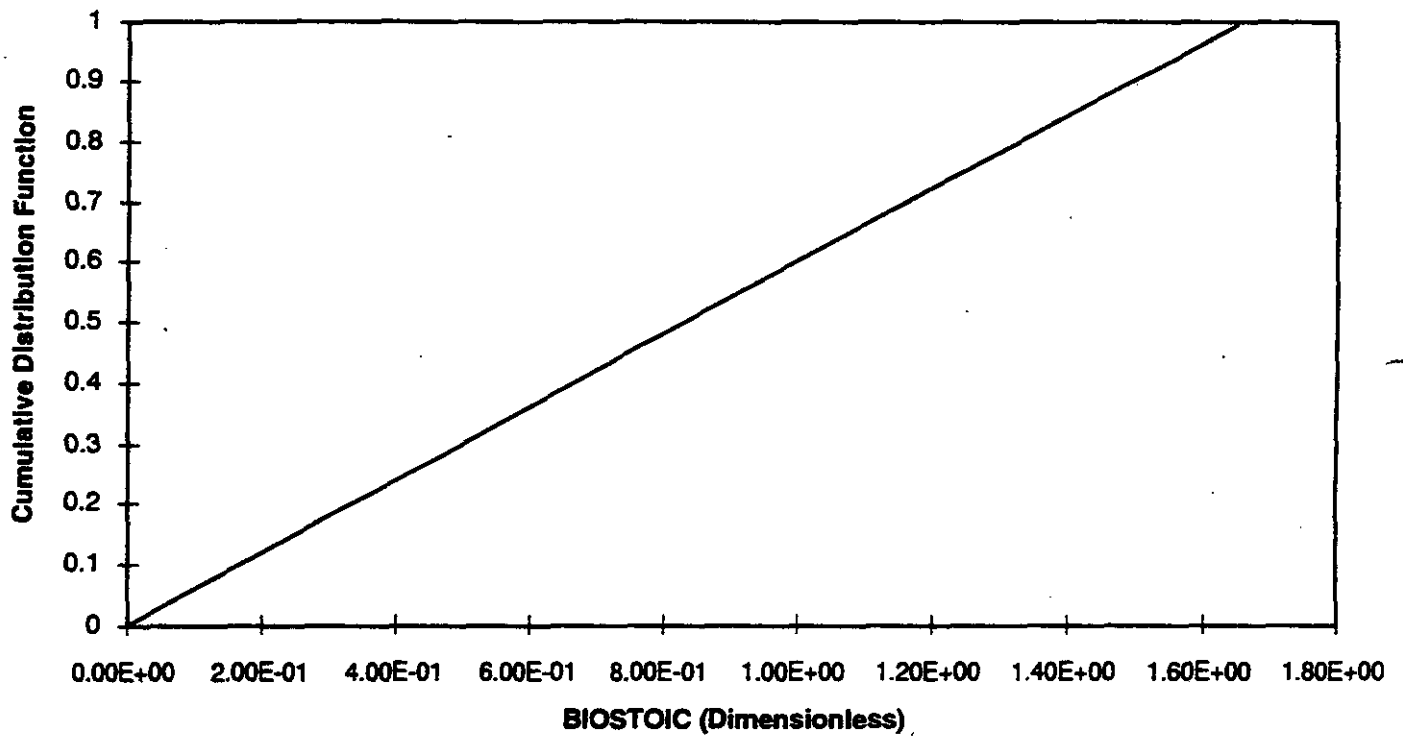


Figure J-1e
Cumulative Distribution Function

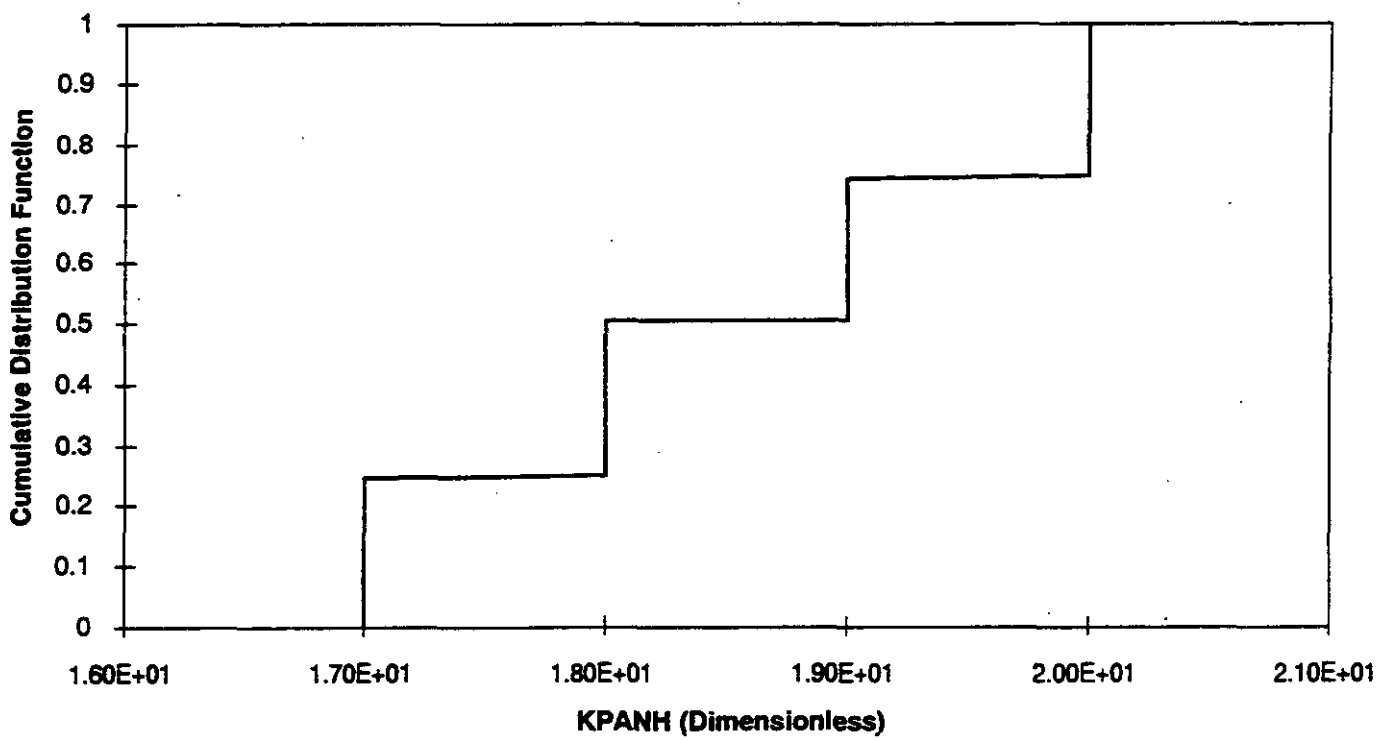
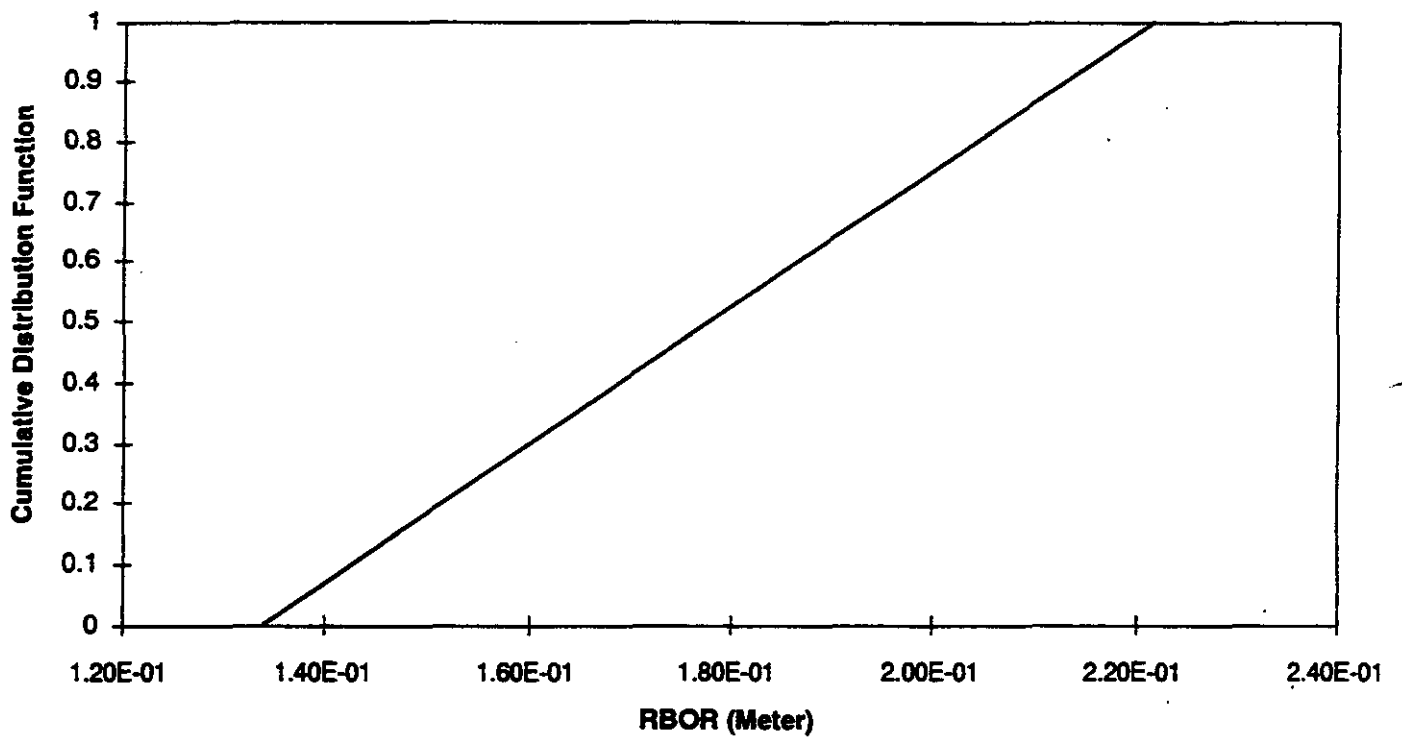
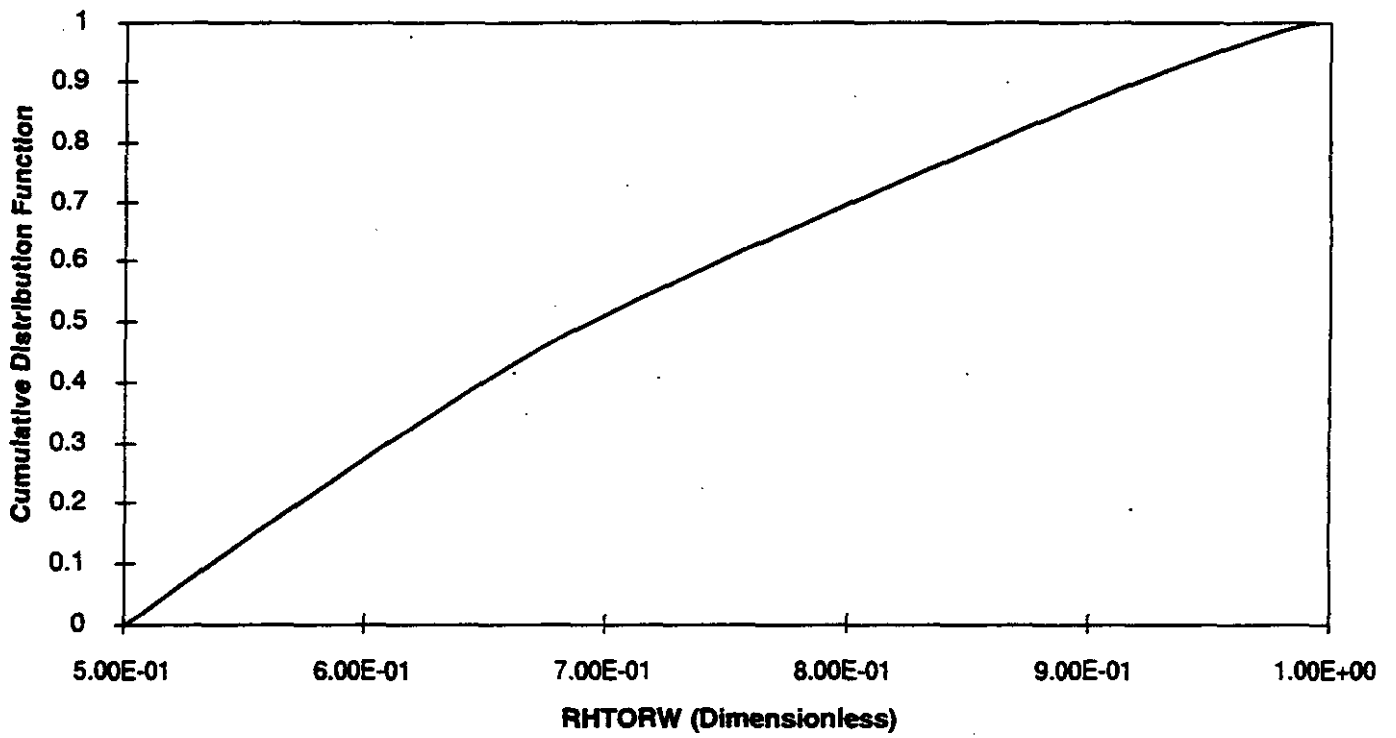


Figure J-1f
Cumulative Distribution Function



M

Figure J-1g
Cumulative Distribution Function



M

Figure J-1h
Cumulative Distribution Function

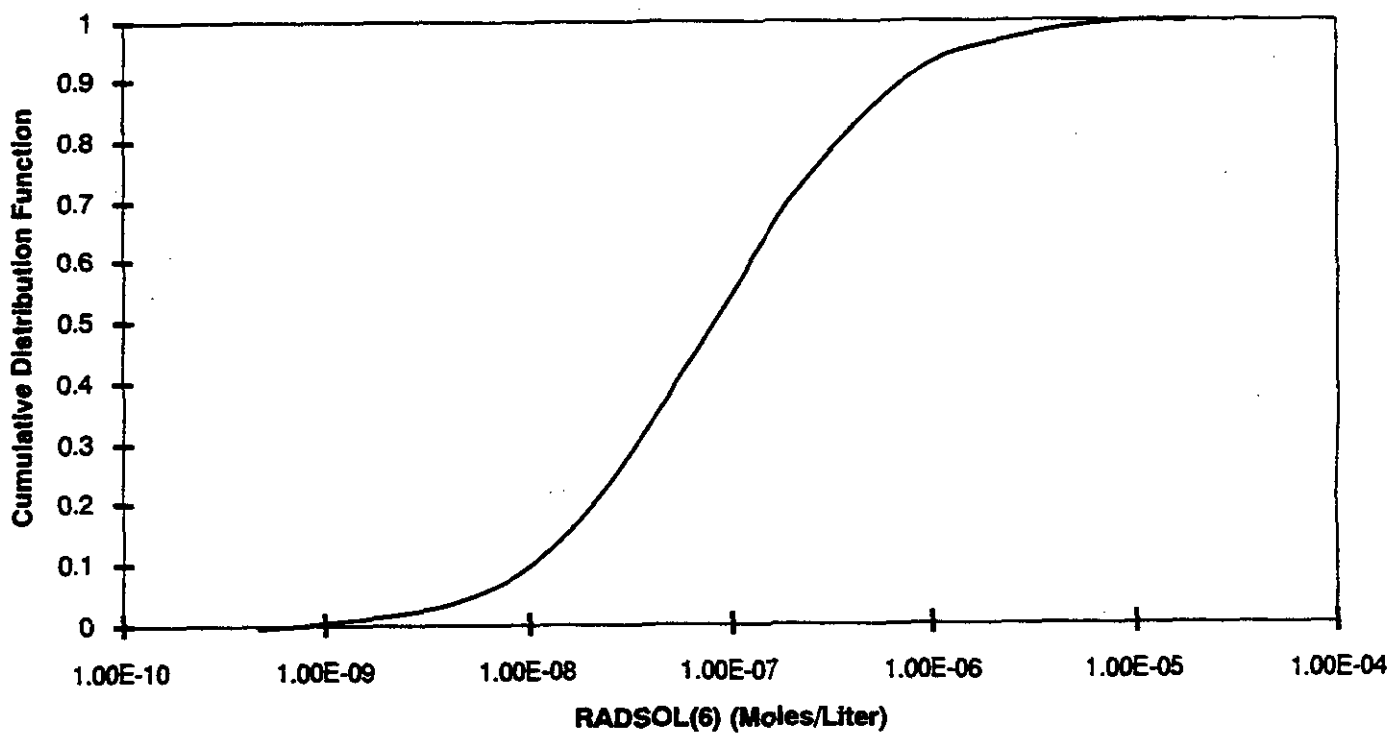
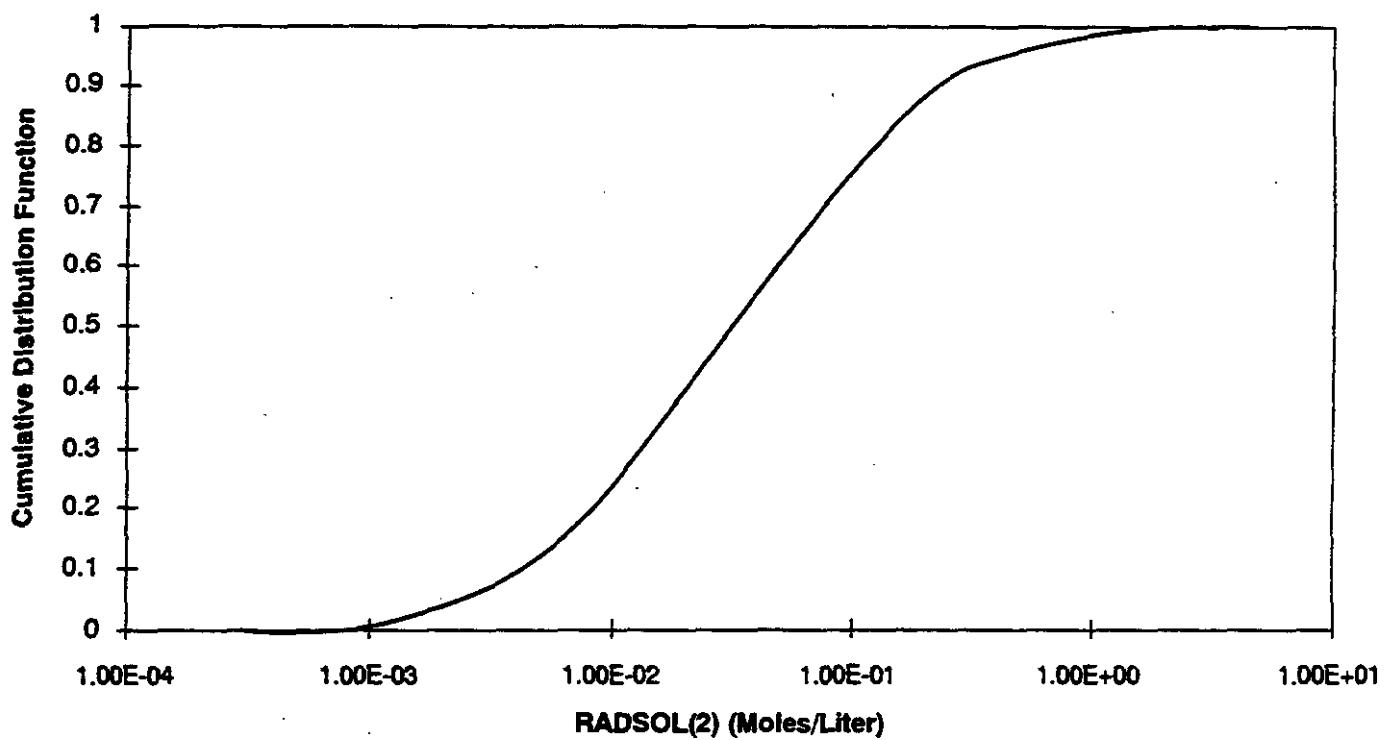
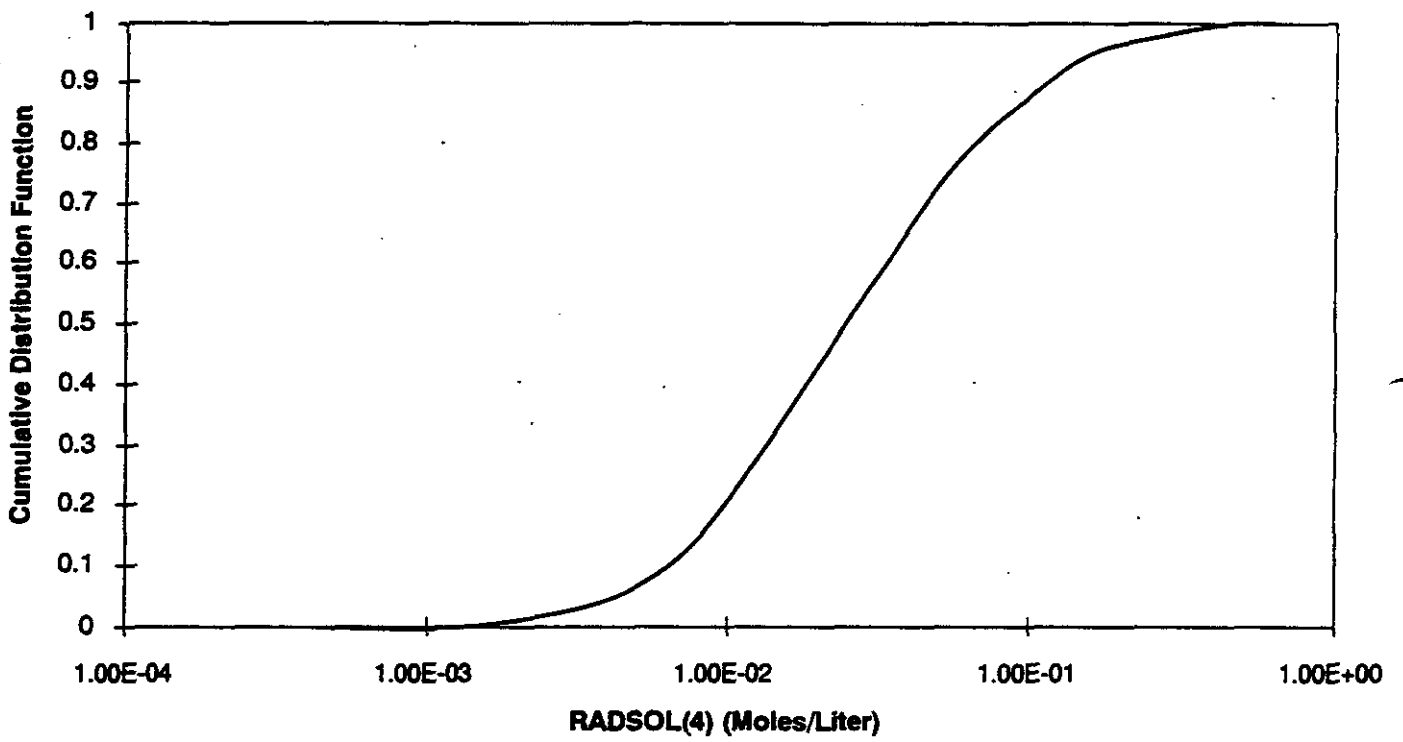


Figure J-1i
Cumulative Distribution Function



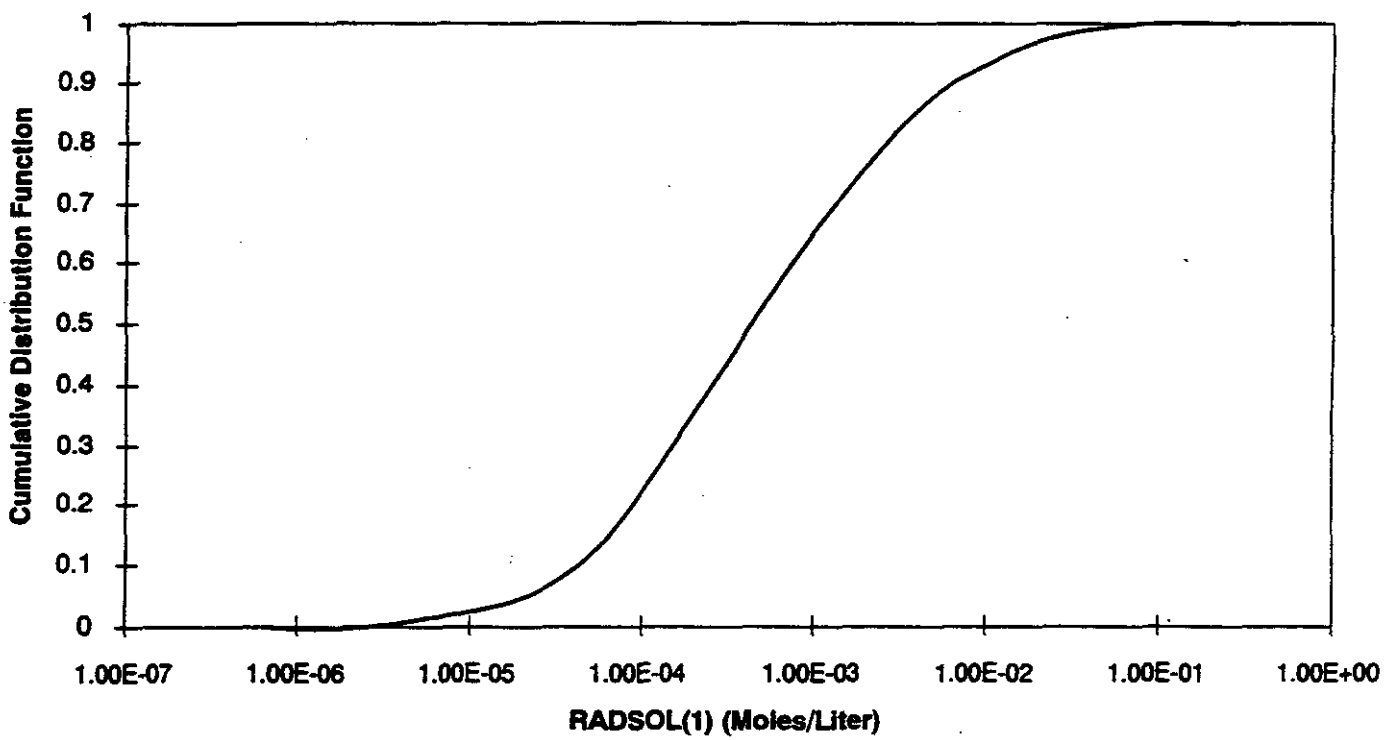
M

Figure J-1j
Cumulative Distribution Function



M

Figure J-1k
Cumulative Distribution Function



M

Figure J-11
Cumulative Distribution Function

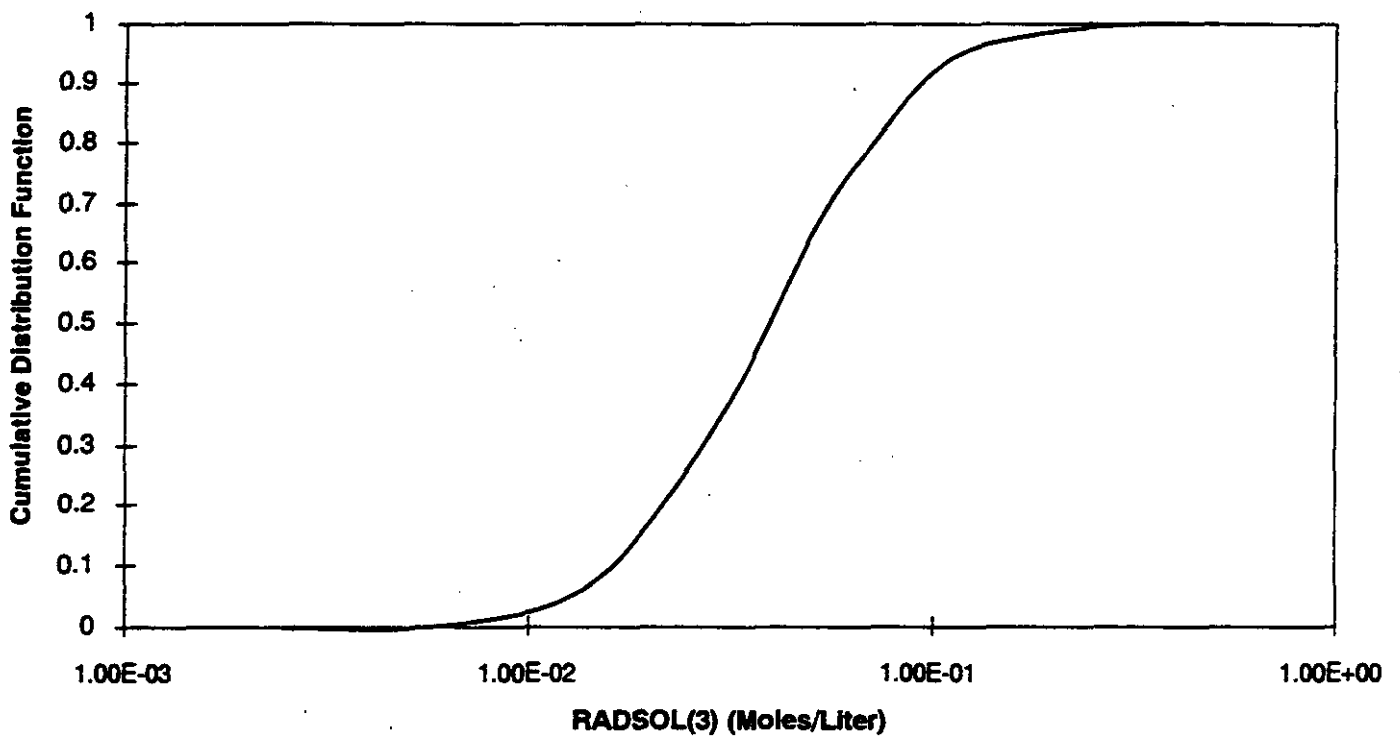


Figure J-1m
Cumulative Distribution Function

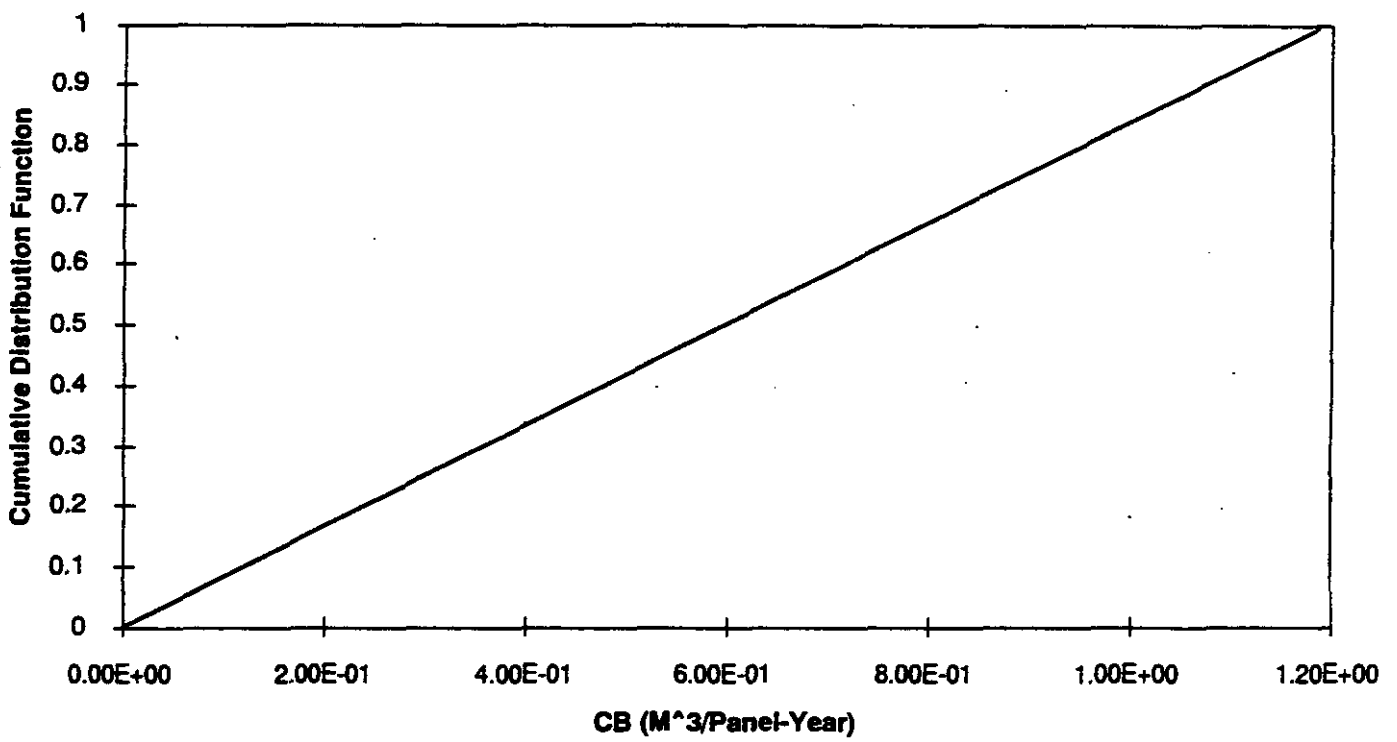


Figure J-1n
Cumulative Distribution Function

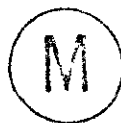
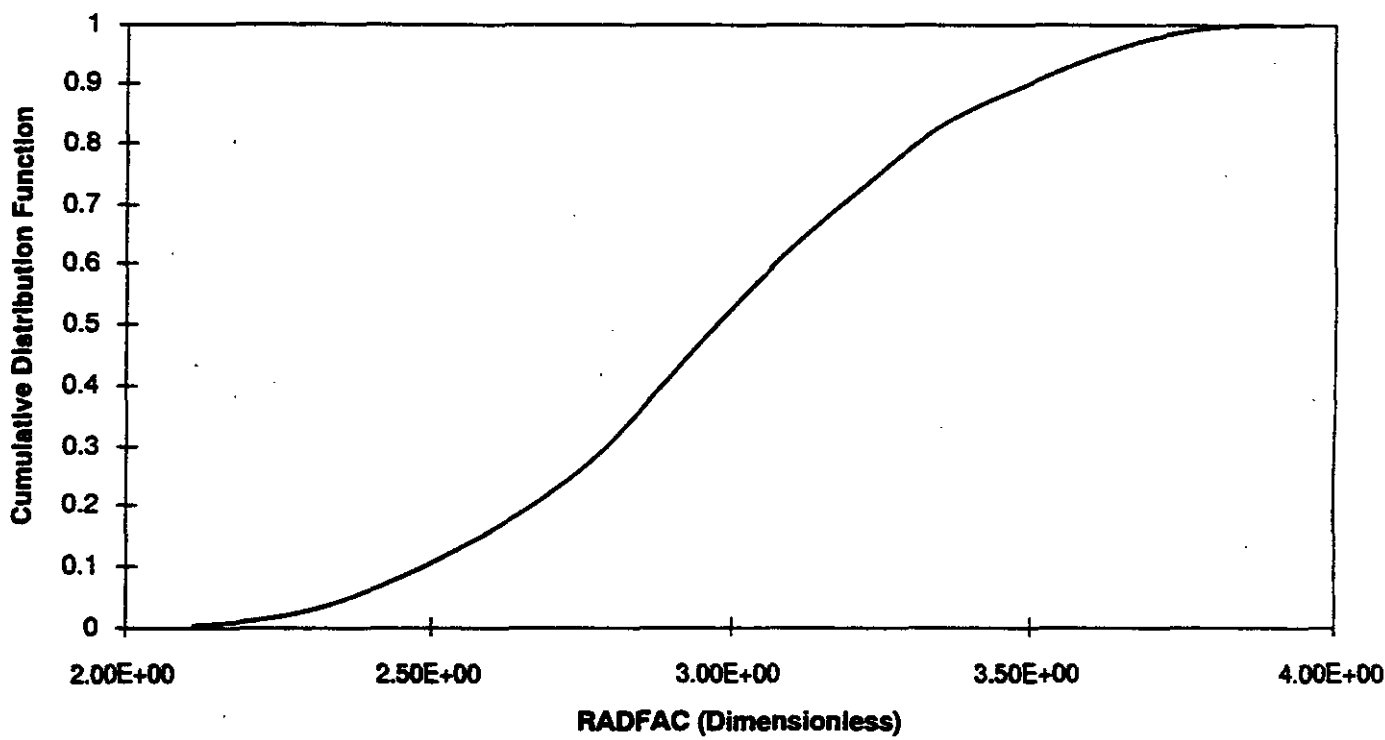
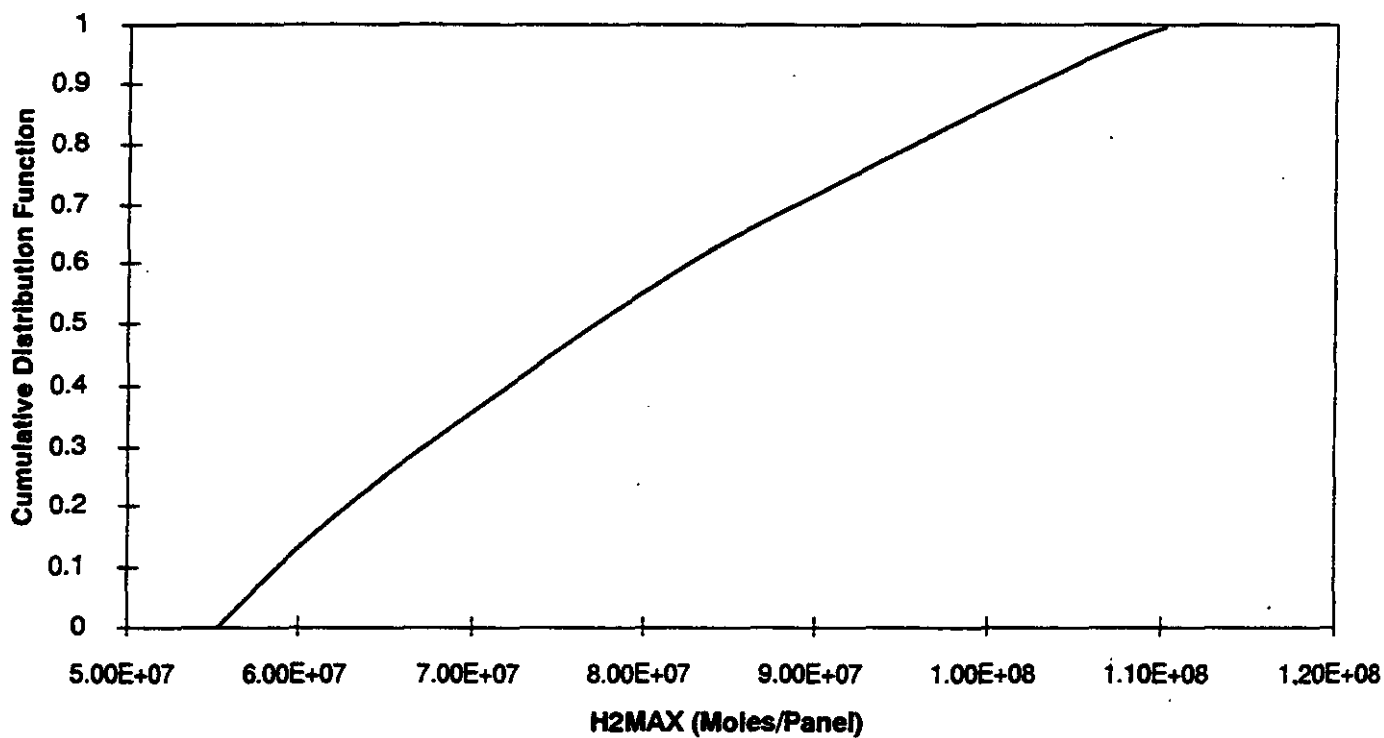


Figure J-1o
Cumulative Distribution Function



M

Figure J-1p
Cumulative Distribution Function

- Different Model for the Rate of the Process. The use of the same random number for the two processes reflects the judgement that the humid gas generation rate should never exceed the inundated biodegradation gas generation rate, since the cumulative distribution of the humid process has lower values at all percentiles of the distribution.
- Solubility of Actinides: The solubility of all the isotopes of a given actinide element are considered to be the same, and the elemental distribution is sampled only once for any given random sample calculation. Individual radioelements are sampled independently.
- Maximum Hydrogen Gas Generation Potential for Anoxic Corrosion (H2MAX): This parameter is calculated by multiplying H2MAX0, the parameter that relates the maximum potential based on metal inventory, and RHTORW, the ratio of the hydrogen gas generation rate to water consumption rate. The parameter H2MAX0 is based on an assumed metallic inventory, and is expressed as a constant. Consequently, the value of H2MAX is totally dependent on the random number used to produce RHTORW.

3.0 IMPACT OF ENGINEERED ALTERNATIVES ON INPUT PARAMETER DISTRIBUTIONS

This section documents the changes to the probability distributions of parameters given in Section 2.0 that result from each engineered alternative. The engineered alternative may also impact best point estimates of input parameters to the DAM whose uncertainties were not modeled. Documentation of the those changes can be found in Appendix E.

Table J-2 identifies the changes made to the uncertain input parameters to reflect the influence of the various EAs. The impacts of these changes are discussed below.

3.1 Changes to H2MAX

Waste processing options that reduce the total number of steel waste containers that would be impacted in a given panel of the Waste Isolation Pilot Plant repository have the potential to reduce the maximum hydrogen gas generation potential from anoxic corrosion. This reduction in potential is reflected by changing the value of H2MAX0, the constant coefficient of the equation that generates the distribution for H2MAX.

Three of the waste processing options have the potential to reduce the number of steel waste containers. Table J-3 below relates the quantities by which the containers would be reduced per room to the reduction in H2MAX0. It should be noted that the values of H2MAX0 do not scale directly with the reduction in equivalent drums, since the mass of contaminated metallic waste and interior metallic containers must also be accounted for.

Figure J-2(a-d) compares the CDF for each of these processing options with that of the baseline value of H2MAX. The net effect of the engineered alternative is to shift the maximum potential anoxic gas generation rate in proportion to the reduction in steel available for the reaction. This



IMPACT OF ENGINEERED ALTERNATIVES ON UNCERTAIN INPUT PARAMETERS IN THE DESIGN ANALYSIS MODEL

Parameters Having Uncertainty	Variable Description (units)	Impact of EA on Probability Distribution															
		1	6	10	33	35a,b	77a	77b	77c	77d	83	94a	94b	94c,d	94e	94f	111
BHUMRATE	Microbial gas generation rate under humid facility conditions (moles/kg cellulose-yr)	No Change From Baseline															
BINURATE	Microbial gas generation rate under inundated facility conditions (moles/kg cellulose-yr)	No Change From Baseline															
BIOSTOIC	Ratio of moles of biogas generated to moles of cellulose consumed (dimensionless)	No Change From Baseline															
CB	Brine inflow rate at a pressure difference of lithostatic minus atmospheric (m ³ /yr-panel)	No Change From Baseline															
H2MAX	Maximum hydrogen gas generation potential from anoxic corrosion (mol/panel)	A	A	A	Baseline	A	A	A	A	No Change from Baseline							
HHUMRATE	Hydrogen gas generation rate from anoxic corrosion under humid facility conditions (moles/drum-yr)	No Change From Baseline															
HINURATE	Hydrogen gas generation rate from anoxic corrosion under inundated facility conditions (moles/drum-yr)	No Change From Baseline															
KPANH	Negative log of the permeability of the anhydrite beds (dimensionless)	No Change from Baseline															
RADFAC	Factor that the drill bit radius (RBOR) is multiplied by to yield an effective radius for use in the cuttings model.	B	B	B	BL	B	B	B	B	B	BL	B	B	B	B	B	BL
RADSOL (1)	Pu-240 solubility in brine (mol/l)	No Change from Baseline								C	C	No Change from BL				C	BL
RADSOL (2)	U-236 solubility in brine (mol/l)	No Change from Baseline								C	C	No Change from BL				C	BL
RADSOL (3)	Am-241 solubility in brine (mol/l)	No Change from Baseline								C	C	No Change from BL				C	BL

AL08-95W/P/EA/CBS/R3744-J

J-23

763435.01 10/12/95 5:33pm

TABLE J-2 (Continued)

IMPACT OF ENGINEERED ALTERNATIVES ON UNCERTAIN INPUT PARAMETERS IN THE DESIGN ANALYSIS MODEL

Parameters Having Uncertainty	Variable Description (units)	Impact of EA on Probability Distribution															
		1	6	10	33	35a,b	77a	77b	77c	77d	83	94a	94b	94c,d	94e	94f	111
RADSOL (4)	Np-237 solubility in brine (mol/l)	No Change from Baseline								C	C	No Change from BL				C	BL
RADSOL (5)	U-233 solubility in brine (mol/l)	Completely Correlated With RADSOL(2)															
RADSOL (6)	Th-229 solubility in brine (mol/l)	No Change from Baseline								C	C	No Change from BL				C	BL
RADSOL (7)	Pu-238 solubility in brine (mol/l)	Completely Correlated With RADSOL(1)															
RADSOL (8)	U-234 solubility in brine (mol/l)	Completely Correlated With RADSOL(2)															
RADSOL (9)	Th-230 solubility in brine (mol/l)	Completely Correlated With RADSOL(4)															
RADSOL (12)	Pu-239 solubility in brine (mol/l)	Completely Correlated With RADSOL(1)															
RBOR	Radius of borehole for intrusion scenarios (m)	No Change From Baseline															
RHTORW	Ratio of hydrogen gas generation rate to water consumption rate during anoxic corrosion (dimensionless)	No Change From Baseline															

Notes:

- BL No Change from Baseline
- A Reflects reduction in the metallic content of waste composite expected to be present with these engineered alternatives.
- B Factor reduced to various degrees to reflect improved strength and toughness of waste composite to resist borehole erosion.
- C Modified to reflect reduced solubility of actinides at as pH moves from 6.1 to 8.3 due to presence of CaO.

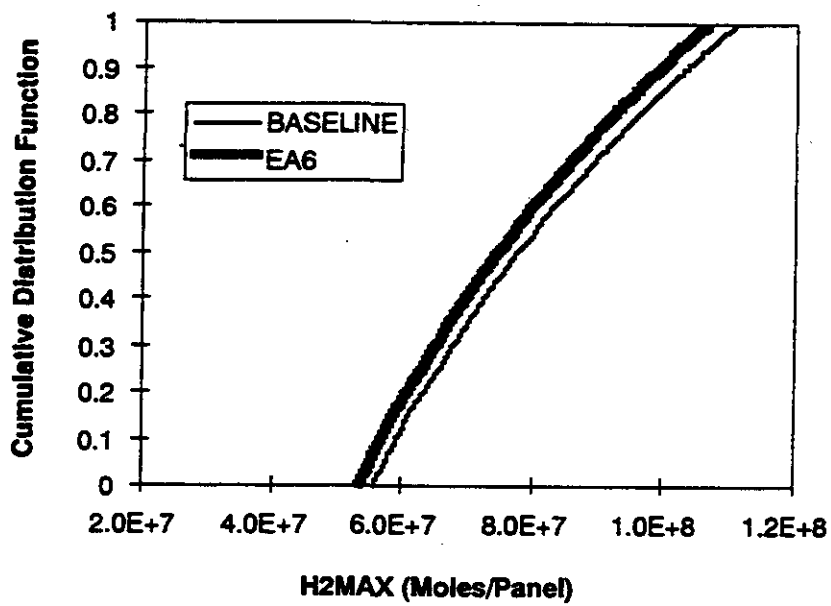


TABLE J-3

**VALUES OF H2MAX0 BASED ON INVENTORIES OF METAL
ASSOCIATED WITH VARIOUS ENGINEERED ALTERNATIVES**

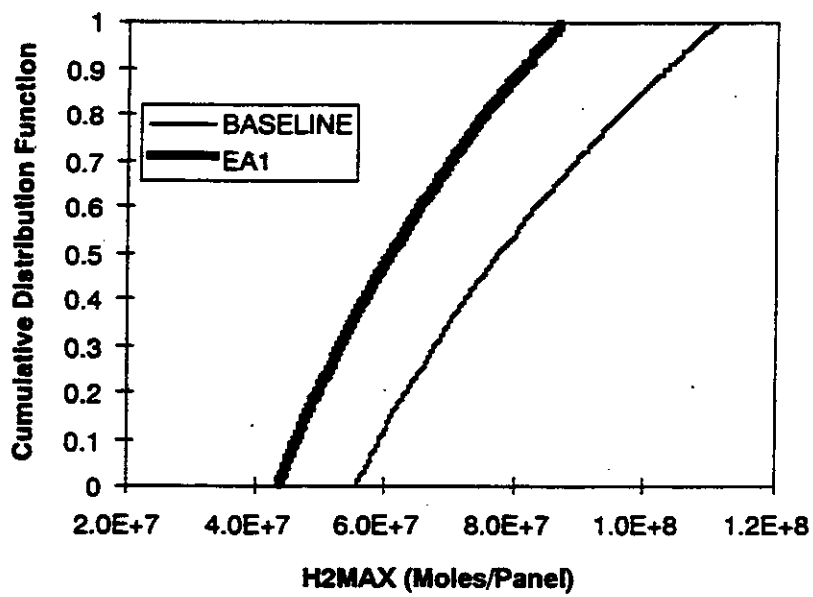
Waste Processing Option	Impacted EAs	Equivalent Number Drums per Room	H2MAX0 (moles/panel)
None	Baseline	6421	7.0E+07
Shred and Compact	6	5381	6.7E+07
Super Compact	1	3604	6.1E+07
Super Compact	77a-d	2000	3.4E+07
Plasma Processing	10	2120	3.7E+07





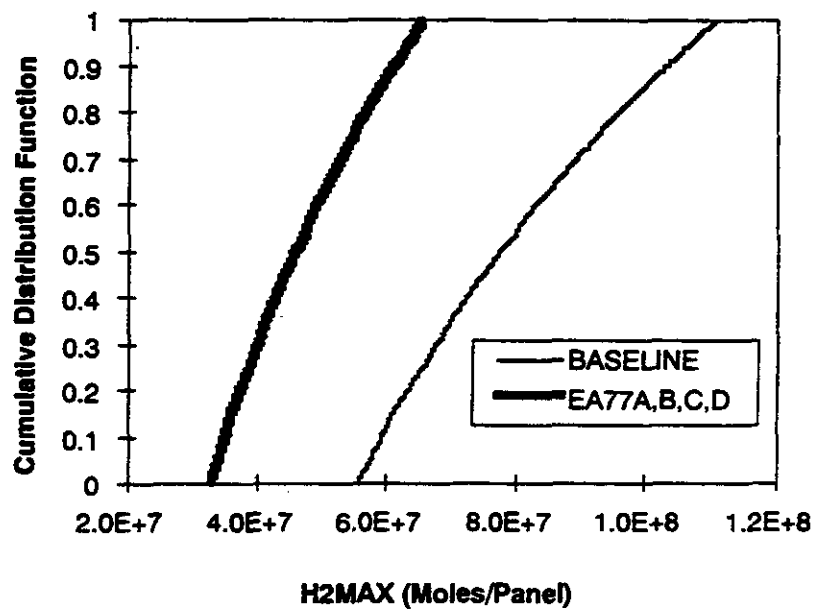
M

Figure J-2a
Uncertainty Distribution of Input Variable H2MAX for EA6



M

Figure J-2b
Uncertainty Distribution of Input Variable H2MAX for EA1



M

Figure J-2c
Uncertainty Distribution of Input Variable H2MAX for EA77A,B,C,D

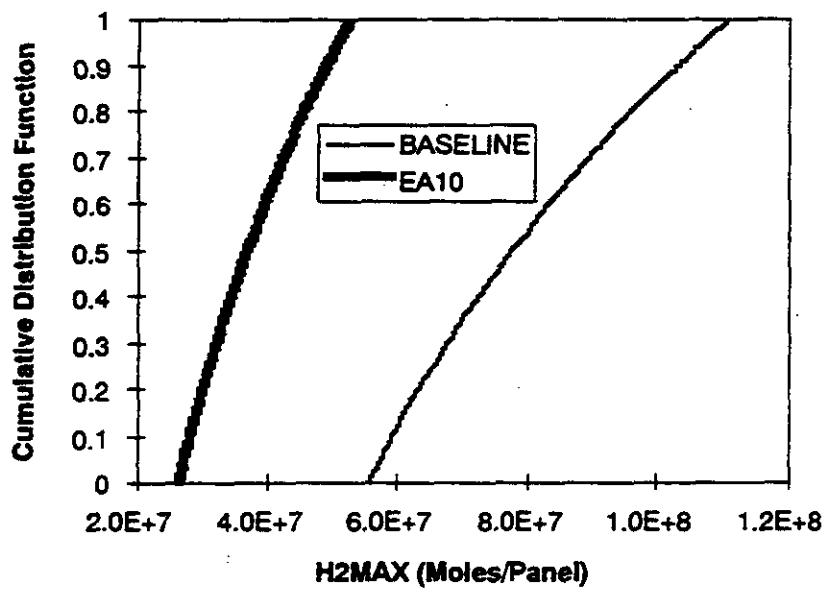


Figure J-2d
 Uncertainty Distribution of Input Variable H2MAX for EA10

1 impact is believed to become important only when there is sufficient water available to totally
 2 react with that quantity of steel.

3
 4 **3.2 Changes to RADFAC**

5
 6 Some EAs improve the shear strength and toughness of the waste/backfill composite that forms
 7 at the waste horizon after consolidation. As a result, these EAs are expected to exhibit enhanced
 8 resistance to enlargement of borehole due to erosion and slurry action during the drilling process.
 9 The first principles model of borehole erosion is still under development in Sandia Performance
 10 Assessment Model. In the absence of available insights from that model, the strength and
 11 toughness of the waste/backfill composite anticipated to be achieved by the various were
 12 grouped and judgmentally ranked from highest to lowest resistance to erosion based on their
 13 anticipated strength and toughness. The variable RADFAC is a factor that the drill bit radius is
 14 multiplied by to determine the effective radius for use in the cuttings release model. The results
 15 of the RADFAC ranking is given in the Table J-4.

TABLE J-4

SUMMARY OF STRENGTH AND TOUGHNESS RANKS FOR ASSESSMENT OF RADFAC

Waste/Backfill Composition	EA Case Number	RADFAC Range	Comments
Solid resulting from Plasma Processing, no backfill	10	50% at 1 50% 1->1.3	If the solid does not degrade it should cut cleanly. Minor erosion if it does degrade.
Supercompacted waste both with and without backfill	1, 77a-d	1.5 ± 30%	Super compaction creates a very dense composite structure
Solids shredded and packed with clay, enhanced sludge cement with cementitious or salt aggregate grout backfill	94c,d	1.75 ± 30%	Combination of enhanced cementation of sludges and grout backfill creates strong composite
No waste processing, but cementitious or salt aggregate grout backfill	35a,b	2.0 ± 30%	Grout backfills increase strength of composite
Solids shredded and packed with clay, enhanced sludge cement, with backfills providing no additional toughness	94a,b,e,f	2.3 ± 30%	Enhanced cementation of sludges provides minor strength increase
Shred and Compact Solid Waste, no backfill	6	2.6 ± 30%	Low-force compaction provides only slight increase in strength of composite
Alternatives providing no additional toughness	33,83	3.0 ± 30%	Resistance to erosion taken to be the same as that used for the baseline design.

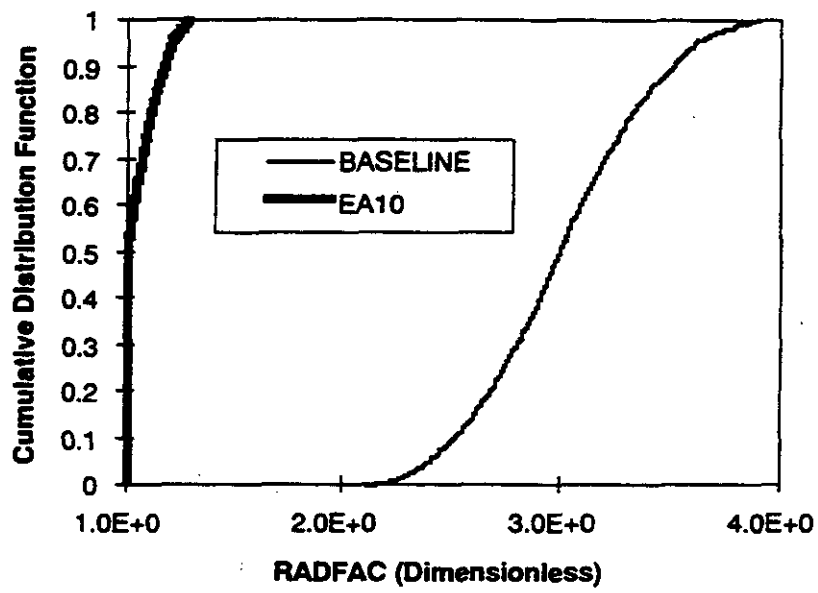


1 Figure J-3(a-f) compares the CDF for each of the modified RADFAC values for with that of the
2 baseline value of RADFAC.
3

4 **3.3 Changes to RADSOL (All Actinide Elements)**
5

6 When lime is used in the backfill of the repository it raises the pH of the brine flowing into waste
7 horizon. The solubility of actinides that the repository is designed to contain are strongly
8 dependent on the pH of the brine. Within the DAM, this impact is modeled by changing the CDFs
9 for the solubility for five elemental actinide solubility from those corresponding to a pH of 6.1 in
10 the baseline to solubilities for a pH of 8.3. The CDFs associated with these solubility changes
11 are shown in Figure J-4(a-e). These changes are based a regression analysis on actinide
12 solubility presented in Appendix H.
13
14





M

Figure J-3a
Uncertainty Distribution of Input Variable RADFAC for EA10

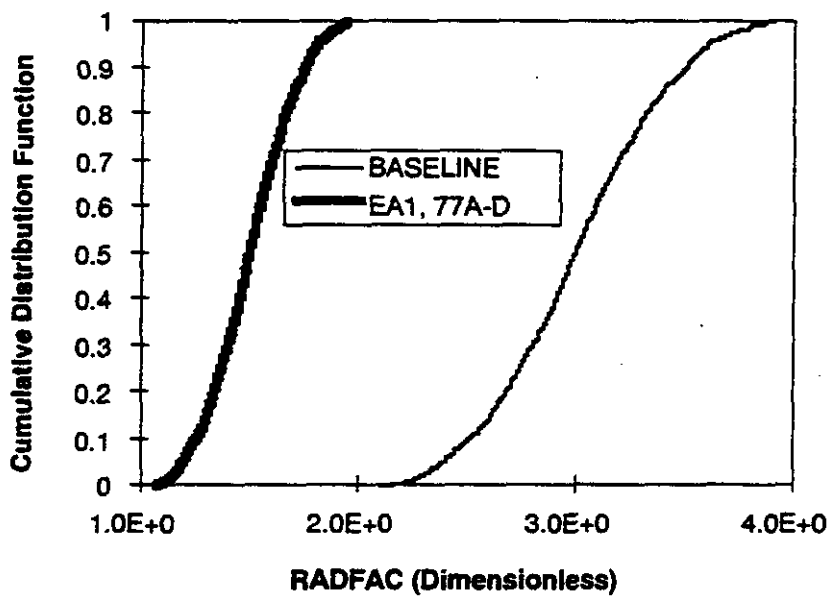
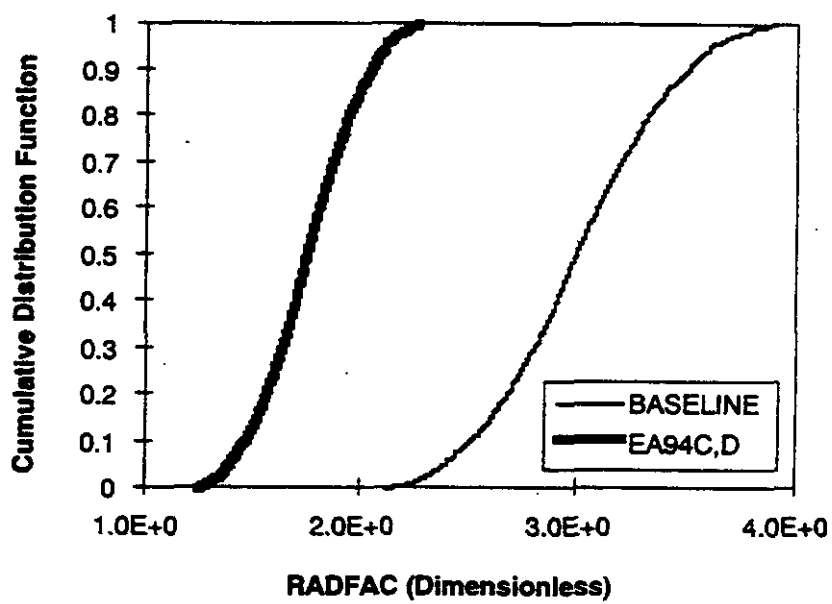


Figure J-3b
Uncertainty Distribution of Input Variable RADFAC for EA1,77A-D



M

Figure J-3c
Uncertainty Distribution of Input Variable RADFAC for EA94C,D

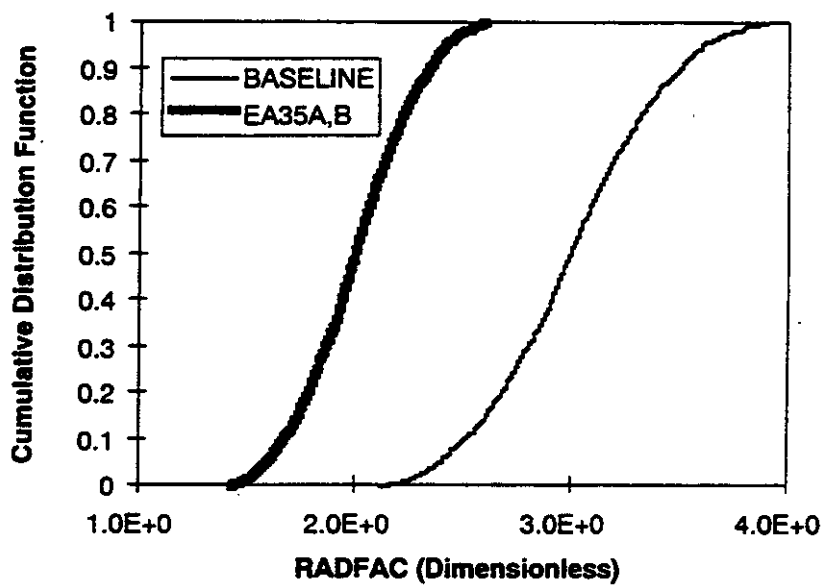


Figure J-3d
Uncertainty Distribution of Input Variable RADFAC for EA35A,B

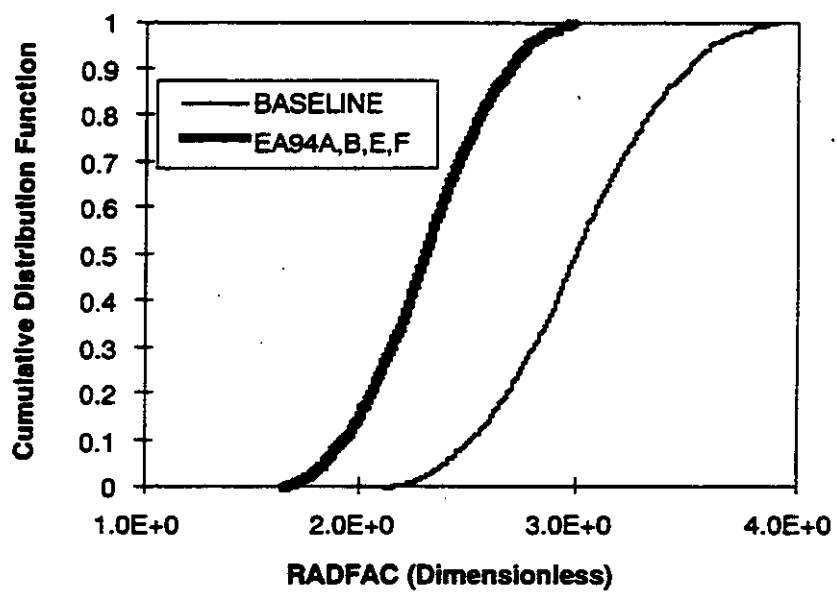


Figure J-3e
Uncertainty Distribution of Input Variable RADFAC for EA94A,B,E,F

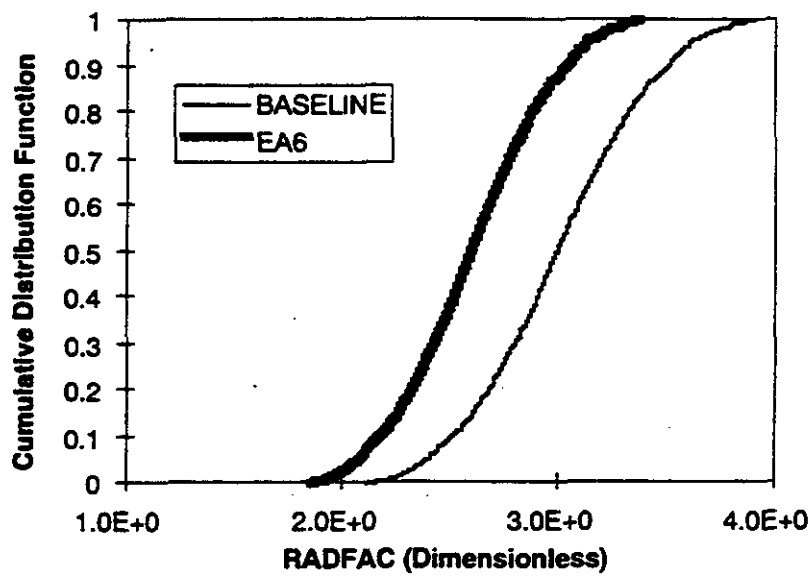


Figure J-3f
Uncertainty Distribution of Input Variable RADFAC for EA6

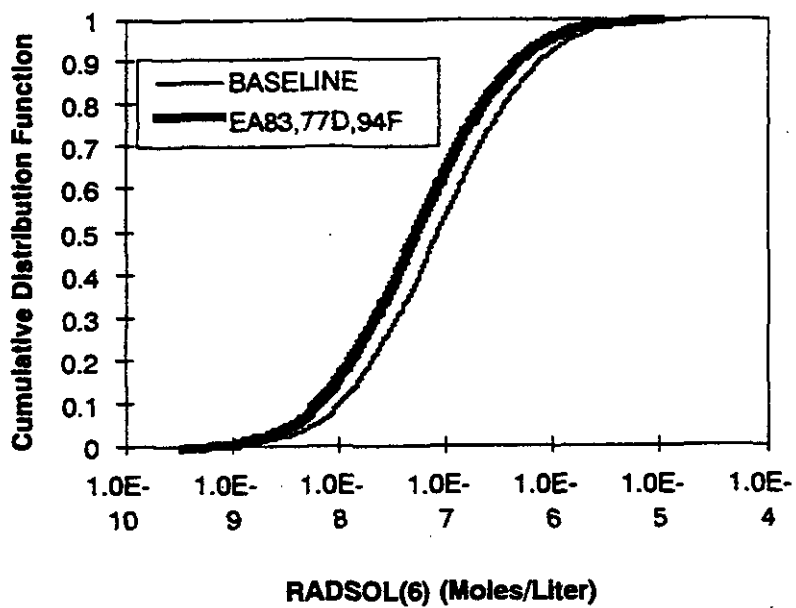


Figure J-4a
Uncertainty Distribution of Input Variable RADSOL(6) for EA83,77D,94F

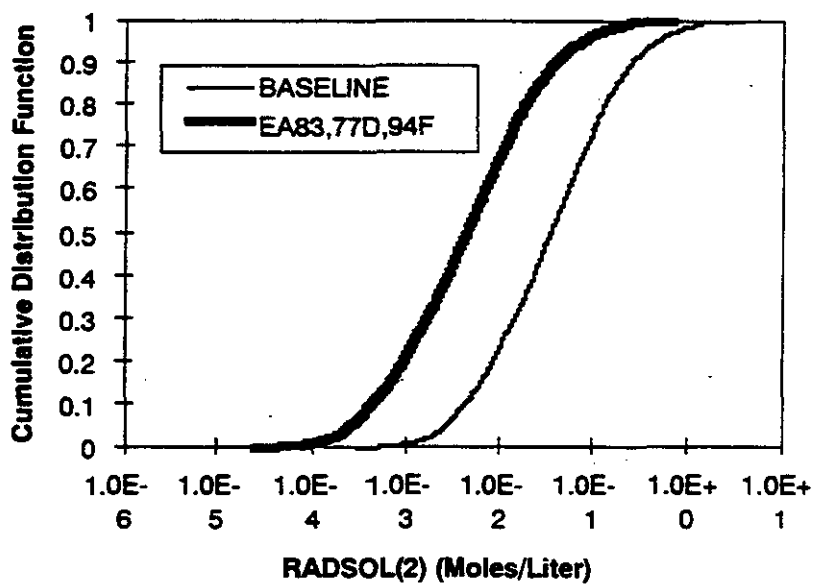


Figure J-4b
Uncertainty Distribution of Input Variable RADSOL(2) for EA83,77D,94F

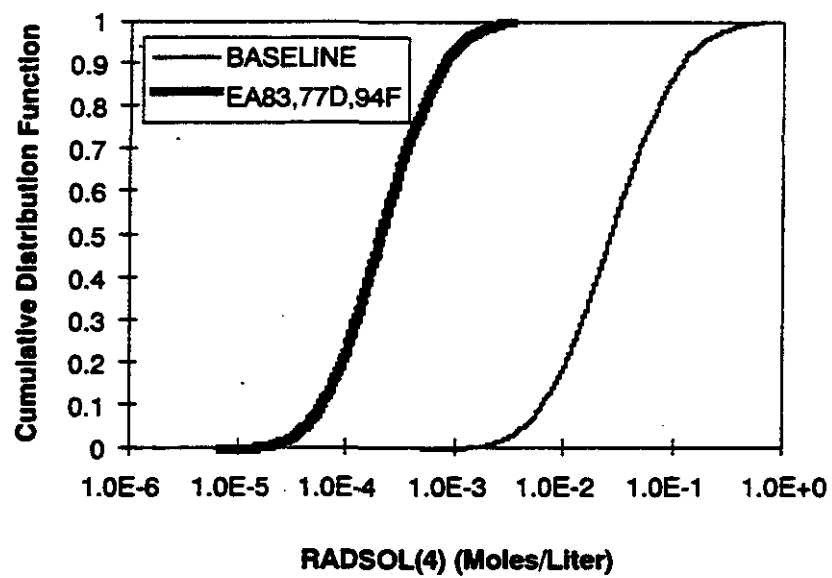


Figure J-4c
Uncertainty Distribution of Input Variable RADSOL(4) for EA83,77D,94F



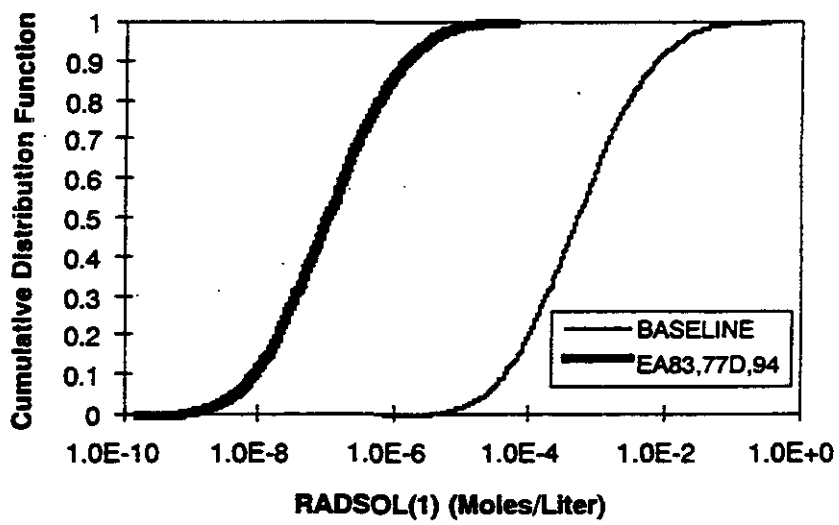


Figure J-4d
Uncertainty Distribution of Input Variable RADSOL(1) for EA83,77D,94F

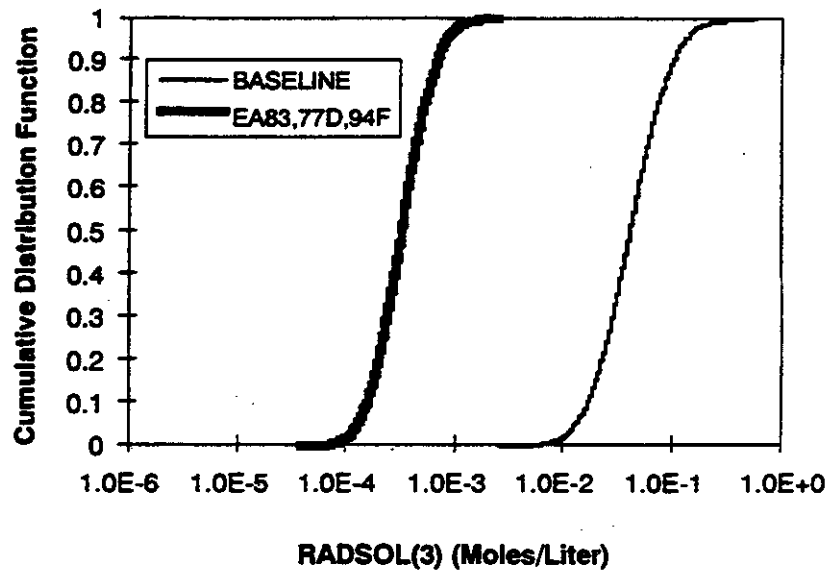


Figure J-4e
Uncertainty Distribution of Input Variable RADSOL(3) for EA83,77D,94F